



**HAL**  
open science

## Computational study of adsorption and the vibrational properties of water on the Cu(110) surface

Lauri Halonen, Elina Sälli, Jukka-Pekka Jalkanen, Kari Laasonen

► **To cite this version:**

Lauri Halonen, Elina Sälli, Jukka-Pekka Jalkanen, Kari Laasonen. Computational study of adsorption and the vibrational properties of water on the Cu(110) surface. *Molecular Physics*, 2007, 105 (09), pp.1271-1282. 10.1080/00268970701420516 . hal-00513104

**HAL Id: hal-00513104**

**<https://hal.science/hal-00513104>**

Submitted on 1 Sep 2010

**HAL** is a multi-disciplinary open access archive for the deposit and dissemination of scientific research documents, whether they are published or not. The documents may come from teaching and research institutions in France or abroad, or from public or private research centers.

L'archive ouverte pluridisciplinaire **HAL**, est destinée au dépôt et à la diffusion de documents scientifiques de niveau recherche, publiés ou non, émanant des établissements d'enseignement et de recherche français ou étrangers, des laboratoires publics ou privés.



**Computational study of adsorption and the vibrational properties of water on the Cu(110) surface**

Journal:	<i>Molecular Physics</i>
Manuscript ID:	TMPH-2007-0006.R2
Manuscript Type:	Full Paper
Date Submitted by the Author:	23-Apr-2007
Complete List of Authors:	Halonen, Lauri; University of Helsinki Sälli, Elina; University of Helsinki, Laboratory of Physical Chemistry Jalkanen, Jukka-Pekka; University of Helsinki Laasonen, Kari; University of Oulu
Keywords:	adsorption, vibrational spectra, variational calculations
<p>Note: The following files were submitted by the author for peer review, but cannot be converted to PDF. You must view these files (e.g. movies) online.</p> <p>artvesi10.tex</p>	



1  
2  
3  
4 Computational study of adsorption and the vibrational  
5  
6  
7 properties of water on the Cu(110) surface  
8  
9  
10

11  
12  
13 ELINA SÄLLI <sup>1</sup>, JUKKA-PEKKA JALKANEN <sup>2</sup>, KARI LAASONEN <sup>3</sup>,  
14  
15 and LAURI HALONEN<sup>1, 4</sup>  
16

17  
18 Laboratory of Physical Chemistry, P.O. Box 55, FIN-00014 University of  
19  
20 Helsinki, Finland  
21

22 Department of Chemistry, P.O. Box 3000, FIN-90014 University of Oulu,  
23  
24 Finland  
25  
26  
27  
28  
29  
30  
31  
32  
33  
34  
35  
36  
37  
38  
39  
40  
41  
42  
43  
44  
45  
46  
47  
48  
49

---

50 <sup>1</sup>University of Helsinki

51 <sup>2</sup>Finnish Meteorological Institute, P.O. Box 503 FIN-00101 Helsinki, Finland

52 <sup>3</sup>University of Oulu

53 <sup>4</sup>Corresponding author. Email: lauri.halonen@helsinki.fi  
54  
55

## Abstract

This work describes adsorption and internal vibrational motion of the water monomer on the Cu(110) surface. We have computed the vibrational wave numbers for the adsorbed water using anharmonic variational calculations previously been applied to the gas phase molecule. The three-dimensional potential energy surface for the vibrational motion of the water molecule has been computed using density functional theory (DFT) with periodic boundary conditions, generalized gradient approximation (GGA), plane wave basis sets and projector augmented wave (PAW) potentials as implemented in the Vienna *ab initio* simulation package (VASP). The data points on the potential energy surface have been fitted into an analytical model and the eigenvalues of the resulting Hamiltonian have been computed variationally.

KEYWORDS: adsorption, vibrational spectra, variational calculations

# 1 Introduction

Vibrational spectra of molecules on the surfaces may be used to identify adsorbed species, distinguish between dissociated, clustered and molecularly adsorbed molecule or study adsorption sites and geometries of the molecule [1], [2]. In addition, the diffusion of molecules, the formation of clusters [3] and surface reactions [4] are assumed to be enhanced by vibrational excitation.

This work describes adsorption of water **monomer** on the Cu(110) surface. We chose the surface plane (110) to represent the copper surface due to the following reasons:

- i The (110) plane is the roughest of the experimentally most studied copper planes (100), (110) and (111) and thus the interaction of water with Cu(110) is stronger than with the flatter Cu(111) or Cu(100) surfaces.
- ii There are experimental data on the vibrational properties of water on the Cu(110) surface.

According to UPS experiments [5], water bonds to the Cu(110) surface through the oxygen lone pair which is in agreement with the work function change  $-1.0$  eV [7]. Adsorption of water through the oxygen end has also been observed in Electron Stimulated Desorption (ESD) study [6] where  $H^+$  was the only ion detected. A comparison [8] between the dipole moment values of the gas phase and the adsorbed water molecule reveals that water uses only one of its free electron pairs for bonding to the metal surface. This is in agreement with UPS results [5] that can be explained if the symmetry

axis of water is nearly parallel to the surface. Andersson [9] *et al.* calculate a tilting angle between the symmetry plane of the water molecule and the normal of the surface to be  $57^\circ$  on the Cu(100) surface based on the intensities of the bending mode and the combined translation-rotation mode in the Electron Energy Loss Spectroscopy (EELS) spectra. Based on the polarization selection rules, Mariani and Horn [10] claim that the adsorption system of water on the Cu(110) surface possesses no symmetry. The bond lengths and bond angle of the water molecule are believed to increase a little in adsorption because the vibrational frequencies of adsorbed water decrease in comparison to the values of the gas phase water molecule [8]. Experimental desorption temperatures of water on the clean Cu(110) surface vary from 160 K to 180 K [11]. Estimates of the adsorption energy or activation energy for desorption vary from  $-0.67$  to  $-0.41$  eV depending on the model used to interpret desorption temperatures.

The vibrational band positions of the water molecule adsorbed on the Cu(110) surface have been studied by High Resolution Electron Energy Loss Spectroscopy (HREELS) [8], [12]. A weak bending mode is observed at  $1600\text{ cm}^{-1}$  and a weak broad OH band around  $3370\text{ cm}^{-1}$  at low coverages. The full-width at half maximum of the stretching band is  $400 - 450\text{ cm}^{-1}$ . It can be separated into three components,  $3180\text{ cm}^{-1}$ ,  $3375\text{ cm}^{-1}$  and  $3600\text{ cm}^{-1}$  when the coverage is increased. These are believed to correspond to the OH stretching bands of OH-bonds hydrogen bonded to the surface, hydrogen bonded to other water molecules and free, respectively. The bending mode is observed at  $1589\text{ cm}^{-1}$  [9],  $1600\text{ cm}^{-1}$  [13] and  $1630\text{ cm}^{-1}$  [14] on the Cu(100) surface. The OH stretching region is observed around

1  
2  
3  
4 3360  $\text{cm}^{-1}$  [14]. On the other hand, a structureless OH-stretching region be-  
5  
6 tween 3230 – 4030  $\text{cm}^{-1}$  has also been reported when the intensity of the  
7  
8 stretching modes has been below the detection limit [9].  
9

10 The development of electronic structure calculations has made it possible  
11  
12 to computationally study detailed properties of molecules adsorbed on metal  
13  
14 surfaces. Ruuska *et al.* [15] have studied the water monomer on the Cu(111)  
15  
16 surface with ten or eight-atomic clusters at the Möller-Plesset (MP2)-theory  
17  
18 level using atomic centered basis sets. The atop site was energetically most  
19  
20 favorable when full-optimization with a ten-atomic cluster was performed.  
21  
22 When a larger 18-atomic cluster model was employed, it was observed that  
23  
24 without the Counter Poise (CP) -correction for the Basis Set Superposi-  
25  
26 tion Error (BSSE) the orientation, where the hydrogen atoms were parallel  
27  
28 to the surface, was energetically the most favorable with adsorption energy  
29  
30  $-0.49$  eV. With the CP correction, the orientation with hydrogens pointing  
31  
32 towards the surface was the most favorable with adsorption energy signifi-  
33  
34 cantly lower,  $-0.16$  eV. Ignaczak *et al.* [16] used cluster models that contain  
35  
36 2 to 12 atoms. Their density functional (DFT) study showed that the atop  
37  
38 site with tilted geometry and tilting angle  $50 - 65^\circ$  and the bridge site with  
39  
40 upright geometry are energetically almost equivalent on the Cu(100) surface  
41  
42 with adsorption energies around  $-0.35$  eV. They do not mention whether  
43  
44 the BSSE correction has been included. Wang *et al.* [17] modeled the copper  
45  
46 planes (100), (110) and (111) with an 18-atomic cluster and studied adsorp-  
47  
48 tion energetics and geometries with DFT. Computed non-BSSE corrected  
49  
50 adsorption energies are  $-0.61$  eV for Cu(111),  $-0.81$  eV for Cu(100) and  
51  
52  $-1.00$  eV for Cu(110). These values are large compared with experimental  
53  
54  
55  
56  
57  
58  
59  
60

1  
2  
3  
4 adsorption energies and other computed values.

5  
6 Periodic boundary conditions with DFT and generalized gradient approx-  
7 imation (GGA) have been used on copper planes (111) [18], [21], (100) [19],  
8 [21] and (110) [20], [21]. All these studied predict the atop site to be the  
9 most favorable one with adsorption energies from  $-0.22$  eV to  $-1.11$  eV. All  
10 adsorption geometries are tilted. The OH-bonds of water are slightly elon-  
11 gated and the bond angles are slightly increased from the gas phase values  
12 on the Cu(100) and Cu(111) surfaces. However, a bond angle as large as  
13  $111^\circ$  has been reported [20] on the Cu(110) surface. The results for the  
14 Cu(100), Cu(110) [21] and Cu(111) surfaces are similar but the adsorption  
15 energies and the bond angles of adsorbed water on the Cu(110) surface [20]  
16 are significantly different. Vibrational frequencies have been calculated on  
17 the Cu(100) surface [22]. In this ab initio work, the surface is modeled with  
18 a five-atomic cluster model and normal mode analysis is used to obtain the  
19 harmonic vibrational frequencies.  
20  
21  
22  
23  
24  
25  
26  
27  
28  
29  
30  
31  
32  
33

34 The aim of this computational work is to study adsorption energetics of  
35 the water monomer on the copper surface, find the preferred adsorption site  
36 and adsorption geometry of the molecule, explain how water bounds to the  
37 surface and model the vibrational motion of the molecule on the surface.  
38 Our variational approach is based on constructing the quantum mechanical  
39 Hamiltonian for the internal vibrational motion and solving the correspond-  
40 ing Schrödinger equation for the vibrational motion. The method is origi-  
41 nally developed for gas phase molecules but as far as we know the model  
42 with all internal vibrational modes included has not been previously applied  
43 to molecules adsorbed on surfaces. In order to keep the number of vibra-  
44  
45  
46  
47  
48  
49  
50  
51  
52  
53  
54  
55

tional degrees of freedom applicable for the variational approach, we restrict the study to a monomeric water molecule and its internal vibrational modes.

We want to answer the following questions: How does the surface influence the vibrational spectra of the molecule compared to a gas phase molecule? How does the adsorption site and adsorption geometry of the molecule affect the vibrational spectra of the molecule? Is there a correspondence between the interaction mechanism between of the adsorption system and the vibrational wave numbers?

## 2 Theoretical and computational model

### 2.1 Vibrational analysis

The vibrational potential energy surface is obtained from electronic structure calculations. This three dimensional vibrational function has been determined by calculating energies on the discrete data points that describe the change of one coordinate or the simultaneous change of two coordinates from the equilibrium geometry. Calculated data points are fitted into an analytical model as explained in chapter 2.3. For the kinetic energy operator, we have used the exact kinetic energy operator for the gas phase water molecule with the equilibrium geometry of the adsorbed molecule. Vibrational kinetic energy operator of the gas phase water molecule is [23]

$$\hat{T}_v = -\frac{\hbar^2}{2} \sum_{ij}^3 \left( \frac{\partial}{\partial q_i} + \frac{1}{J} \frac{\partial J}{\partial q_i} \right) g^{(q_i, q_j)} \frac{\partial}{\partial q_j} \quad (1)$$

where coordinates  $q_i$  are displacements from the equilibrium bond length,  $\Delta r_1$ ,  $\Delta r_2$  and the displacement from the bond angle  $\Delta \theta$  and  $g$ -matrix ele-

ments are given by

$$q^{(q_i, q_j)} = \sum_{\alpha=1}^3 \frac{1}{m_\alpha} (\nabla_\alpha q_i) \cdot (\nabla_\alpha q_j). \quad (2)$$

The volume element of integration needed to calculate matrix elements  $\int d\tau \psi \hat{T}_v \psi$  and  $\int d\tau \psi \hat{V}_v \psi$  is

$$d\tau = J dr_1 dr_2 d\theta \quad (3)$$

where the Jacobian of the coordinate transformation is

$$J = |\det g^{(q_i, q_j)}|^{-\frac{1}{2}} \prod_{\alpha=1}^3 m_\alpha^{-\frac{3}{2}}. \quad (4)$$

We have applied an appropriate unitary similarity transformation to the kinetic energy operator in order to have a unit weight factor  $J$  in the volume element [23]. The g-matrix elements are presented, for example, in reference [24]. The eigenvalues of the vibrational Hamiltonian have been obtained variationally.

The use of the exact kinetic energy operator is based on the assumption that the surface perturbs the potential energy surface of the molecule and its equilibrium geometry only. In practice, the metal surface perturbs the adsorbed molecule and changes its translational and rotational degrees of freedom into low-frequency vibrations that are called frustrated translations and rotations [1]. In addition, the phonon modes of the metal surface may couple to other vibrational modes. On the Cu(110) surface, the hindered translation and libration modes have been observed at 460 and 745  $\text{cm}^{-1}$  by HREELS [8], [12]. These values are low compared with high-frequency modes of water as the bending mode at 1600  $\text{cm}^{-1}$  is the lowest of them. We assume that the ordinary vibrational modes of the molecule are uncoupled to

1  
2  
3  
4 the translational and rotational vibrations. Therefore, we can use the exact  
5 gas phase kinetic energy operator for the adsorbed molecule. Our assumption  
6 is justified by the difference of these wave numbers [25]. The same adiabatic  
7 assumption has previously been applied to ammonia adsorbed on the Ni(111)  
8 surface [26] and tested in the case of the possible coupling of the N – Ni  
9 stretching and N – H stretching.  
10  
11  
12  
13  
14  
15  
16  
17

## 18 2.2 Electronic structure calculations

19  
20 Electronic structure calculations were required for relaxations of the isolated  
21 water molecule, the copper(110) surface and the water-surface system. All  
22 calculations were performed using Vasp (Vienna *ab initio* simulation package)  
23 [27]. It is a code for electronic structure calculations and molecular dynamics  
24 simulations in solid state materials but it can also be applied to surface  
25 calculations with a slab model.  
26  
27  
28  
29  
30  
31

32 Calculations were based on the density functional theory (DFT) with the  
33 generalized gradient approximation (GGA) of Perdew and Wang (PW91),  
34 PAW pseudo potentials [28] and plane wave basis sets as implemented in  
35 Vasp. The energy cut-off for plane waves was 520 eV. Fermi level was  
36 smeared by the 2nd order Methfessel-Paxton method with a width of 0.4 eV.  
37 All calculations were spin restricted. Electronic energy was converged to  
38 at least  $10^{-4}$  eV in all calculations. For the  $k$ -point sampling of the Brillouin  
39 zone for integrations, the Monkhorst-Pack  $k$ -mesh 441 (16 irreducible  
40  $k$ -points) was employed for relaxations when we tried to find the most fa-  
41 vorable adsorption site and geometry for the adsorbed water molecule. A  
42 denser Monkhorst-Pack  $k$ -mesh 661 (36 irreducible  $k$ -points) was chosen for  
43  
44  
45  
46  
47  
48  
49  
50  
51  
52  
53  
54  
55  
56  
57  
58  
59  
60

1  
2  
3  
4 the final relaxations of the water-surface system.

5  
6 Modeling of the gas phase water molecule needed to be done with ar-  
7  
8 tificial periodicity because of the plane wave code employed. The isolated  
9  
10 water molecule was placed inside a cubic super cell with dimensions of 10 Å.  
11  
12 Only one  $k$ -point (the gamma point) was used in integrations because the  
13  
14 periodicity was artificial. The copper(110) surface was modeled with the slab  
15  
16 model: five layers of metal atoms with four atoms in each layer and a vac-  
17  
18 uum region of 10 Å between the layers. A theoretical lattice constant value  
19  
20 of 3.63 Å obtained in our calculations was used instead of the experimental  
21  
22 one 3.61 Å [29]. The reconstruction of the bare surface decreased the lattice  
23  
24 constant in the direction of the surface normal close to the surface by 9 %  
25  
26 compared with the calculated bulk lattice constant. The adsorbed molecule  
27  
28 was placed on one side of the slab and periodic boundary conditions were  
29  
30 used to multiply the super cell in three dimensions as shown in figure 1.

31  
32 Conjugate gradient and quasi-Newton methods were employed in the  
33  
34 structural searches. The water molecule and the two uppermost layers of  
35  
36 the copper surface were relaxed while the bottom layers were fixed at their  
37  
38 bulk positions until the Hellman Feynman forces on all relaxed atoms were  
39  
40 less than  $0.05 \text{ eV } \text{Å}^{-1}$ . A stricter value  $0.005 \text{ eV } \text{Å}^{-1}$  was used in the final  
41  
42 relaxations.

43  
44 For each discrete data point on the potential energy surface of the in-  
45  
46 ternal coordinates of the water molecule, only the degrees of freedom that  
47  
48 correspond the studied part of the potential energy surface were changed.  
49  
50 The metal surface and the coordinates of the water molecule with respect  
51  
52 to the surface were fixed at their equilibrium positions. We found that the

1  
2  
3  
4 definition of the bending motion was not obvious. There is a unique defini-  
5 tion of the bending coordinate for a gas phase molecule [30]. For a molecule  
6 adsorbed on the surface, this coordinate is mixed with coordinates that de-  
7 scribe hindered rotations with respect to the surface. We decided to test this  
8 by computing the total energies of the asymmetrically adsorbed molecule by  
9 performing bending by moving one of the hydrogens only, moving the other  
10 hydrogen atom only and moving both hydrogens equally so that the approx-  
11 imate direction of the symmetry axis of the water molecule was kept fixed.  
12 The effect of the choice of the bending coordinate was found insignificant.  
13 Eventually, we defined the bending coordinate to satisfy the latter condition.  
14  
15  
16  
17  
18  
19  
20  
21  
22  
23

### 2.3 The potential energy surface

24  
25 Morse coordinates  $y_i = 1 - e^{-a\Delta r_i}$  were used as coordinates for the stretches  
26 instead of displacement coordinates  $\Delta r_i = r_i - r_i(eq)$  from the equilibrium  
27 bond length  $r_i(eq)$ . Direct displacement coordinates  $\Delta\theta = \theta - \theta(eq)$  from  
28 the equilibrium bond angle  $\theta(eq)$  were used for the bending. The potential  
29 energy function used is similar to one in Ref [31]. In all the fits, the potential  
30 energy parameters were optimized with the non-linear least-square method  
31 using MATHEMATICA.  
32  
33  
34  
35  
36  
37  
38  
39  
40  
41

42 Twelve data points from  $-0.4$  to  $1.2$  Å on the stretching part of the po-  
43 tential were fitted into a potential energy model  
44  
45

$$D_2 y_1^2 + D_3 y_1^3 + D_4 y_1^4 \quad (5)$$

46  
47 where we denote parameters for one OH-bond by  $D_2$ ,  $D_3$  and  $D_4$  and  $D'_2$ ,  $D'_3$   
48 and  $D'_4$  for the other one. The value of the Morse parameter  $a$  ( $a'$  for the other  
49 one) obtained was used as a parameter in the following fits. For the isolated  
50  
51  
52  
53  
54  
55

water molecule, the symmetric and upright adsorption geometry, only one stretching curve was computed because the bonds are identical, whereas for the asymmetric adsorption geometry the data points were computed for both bonds and two sets of parameters were optimized.

The bending curve was determined using 13 data points in the range  $50^\circ < \theta < 180^\circ$  and the points were fitted into the potential energy function

$$C + \frac{1}{2}f_{\theta\theta}\Delta\theta^2 + \frac{1}{6}f_{\theta\theta\theta}\Delta\theta^3 + \frac{1}{24}f_{\theta\theta\theta\theta}\Delta\theta^4 \quad (6)$$

where  $C$  and  $f_i$  are parameters.

The potential energy coupling between two bond oscillators was calculated using 16 data points from  $-0.2 \text{ \AA}$  to  $0.2 \text{ \AA}$  and the potential energy coupling between the bending and stretching motions was calculated with 16 points from  $-0.2 \text{ \AA}$  to  $0.2 \text{ \AA}$  and  $90^\circ$  to  $120^\circ$ . The energies were fitted into potential energy function

$$E(\Delta r_1, \Delta r_2, 0) = E(\Delta r_1, 0, 0) + E(0, \Delta r_2, 0) + E(0, 0, 0) + (aa')^{-1}f_{rr'}y_1y_2 \quad (7)$$

where a harmonic force constant  $f_{rr'}$  describes strength of the interaction. By  $E(\Delta r_1, \Delta r_2, \Delta\theta)$  we denote energy of a data point with stretches  $\Delta r_1$  and  $\Delta r_2$  and bond angle displacement  $\Delta\theta$ . The coupling points of bending and stretching were fitted into analytical model

$$E(\Delta r_1, 0, \Delta\theta) = E(\Delta r_1, 0, 0) + E(0, 0, \Delta\theta) + E(0, 0, 0) + a^{-1}f_{r\theta}y_1\Delta\theta + \frac{1}{2}a^{-1}f_{r\theta\theta}y_1\Delta\theta^2 + \frac{1}{2}(a^{-2}f_{rr\theta} + a^{-1}f_{r\theta})y_1^2\Delta\theta, \quad (8)$$

where  $f_i$  force constants describe the strength of the bend-stretch interaction.

The effect of changing the bond angle and the bond lengths at the same time was tested and found to have such a small effect on the vibrational wave

1  
2  
3  
4 numbers that the appropriate potential energy terms were omitted from  
5  
6 this work.  
7  
8

## 9 10 **2.4 Variational calculations**

11  
12 Vibrational wave numbers were obtained variationally with a program origi-  
13 nally written for the symmetric water molecule and modified for this problem  
14 where the water molecule possesses asymmetric structure. The matrix ele-  
15 ments were calculated either with analytical formulas or numerically with  
16 Gauss-Hermite and Gauss-Laguerre numerical integration methods. See ref.  
17 [31] and [32] for more details. Products of harmonic oscillator eigenfunctions  
18 for the bend and Morse oscillator eigenfunctions for the stretches were used  
19 as basis functions. All the bending and stretching states up to seven quanta  
20 were included. The convergence with respect to the to the number of inte-  
21 gration points and the size of the basis set was tested in the case of the gas  
22 phase water using variational program for the symmetric water where more  
23 basis functions were available in the program. A convergence better than  
24  $0.1 \text{ cm}^{-1}$  was achieved for all reported transitions.  
25  
26  
27  
28  
29  
30  
31  
32  
33  
34  
35  
36  
37  
38  
39  
40

## 41 **3 Results and discussion**

### 42 43 44 **3.1 Convergence tests**

45  
46  
47 Convergence tests were performed with respect to the size of the  $k$ -point  
48 mesh, cut-off energy, the width of the Fermi level smearing, spin polarization  
49 and the size of the super cell for the most favorable symmetric adsorption  
50 geometry. Results showed that convergence with respect to the adsorption  
51  
52  
53  
54  
55

1  
2  
3  
4 energy is obtained within 3 % and with respect to the structural parameters  
5  
6 at least within 8 %. The  $k$ -point mesh 881 (32 non-reduced points) and  
7  
8 661 (18 non-reduced points) gave identical results excluding tilting angle  
9  
10 whereas there is a small numerical difference between the  $k$ -point mesh 441  
11  
12 (8 non-reduced  $k$ -points) and 661. The difference was small and therefore  
13  
14 the  $k$ -point mesh 441 was used in finding the adsorption geometry and 661  
15  
16 only for final relaxations. Cut-off energy 800 eV gave the same results as the  
17  
18 cut-off energy 520 eV. Spin-polarization had no effect on the geometry and  
19  
20 only small effect on adsorption energy. However, the energy difference was  
21  
22 too small to require more expensive spin-unrestricted calculations. We found  
23  
24 out that the size of the super cell has clearly more effect on the adsorption  
25  
26 geometry and energetics than any of the computational parameter. Results  
27  
28 of the convergence tests with respect to the size of the super cell are presented  
29  
30 in table 1.

31  
32 Although  $2 \times 2$  and  $3 \times 3$  slabs with coverages 0.25 and 0.11 gave ac-  
33  
34 ceptable adsorption energies, we also studied the possibility of direct lat-  
35  
36 eral interactions between water molecules by computing energies of water  
37  
38 molecules inside the super cells that had been used in surface calculations  
39  
40 without the surface. We used  $k$ -point mesh 661 instead of a gamma point  
41  
42 for  $k$ -space integrations to allow the interaction between neighboring cells.  
43  
44 Energy difference was 0.002 eV.  
45  
46  
47  
48  
49  
50  
51  
52  
53  
54  
55

### 3.2 Adsorption energetics and mechanism of water on the Cu(110) surface

There are four adsorption sites of high symmetry on the (110) surface of the fcc metal : an atop site right above a copper atom of the first layer, large and short bridge sites between the copper atoms of the first layer and a hollow site above a copper atom on a second layer. In addition, the direction of copper rows defines symmetric geometries on these sites yielding ten symmetric adsorption geometries.

We calculated first adsorption energy and geometry on the symmetric adsorption geometries. We employed an assumption that water bounds to the surface through the oxygen atom as suggested by [33]. However, all the coordinates of the water molecule were allowed to relax. It was found that the most favorable adsorption site is atop and the adsorption geometry is tilted with respect to the surface. Then we performed a few tests with asymmetric geometries and found out that a lower adsorption energy was achieved when adsorption geometry is asymmetric. We continued with non-symmetric adsorption geometries and tested eleven non-equivalent asymmetric initial adsorption geometries. We chose these initial geometries so that the oxygen atom was on the atop site and the bond lengths and the bond angle of water corresponded to the gas phase values of water. The resulting geometries were such that either both hydrogens point away from the surface or one hydrogen points away from the surface and the other is almost parallel to the surface or directed to the surface. Eight of these eleven initial geometries produced an asymmetric adsorption geometry that was energetically most favorable. Finally we performed relaxations with convergence criteria  $0.005 \text{ eV}\text{\AA}^{-1}$  for

1  
2  
3  
4 forces and a  $k$ -point mesh 661 for this most favorable asymmetric adsorption  
5  
6 geometry and the most favorable symmetric adsorption geometry.  
7

8 The computational adsorption energy is defined as  $E_a = E_{rel}(\text{H}_2\text{O} + \text{Cu}) -$   
9  
10  $E_{rel}(\text{H}_2\text{O}) - E_{rel}(\text{Cu})$ , where  $E_{rel}(\text{H}_2\text{O} + \text{Cu})$ ,  $E_{rel}(\text{H}_2\text{O})$  and  $E_{rel}(\text{Cu})$  are the  
11  
12 energies of the relaxed water-copper system, relaxed isolated water molecule  
13  
14 and relaxed copper surface, respectively. Symmetric and asymmetric adsorp-  
15  
16 tion geometries are almost equivalent energetically although the asymmetric  
17  
18 geometry is slightly more favorable with an adsorption energy of  $-0.36$  eV  
19  
20 than the symmetric adsorption geometry that possesses an adsorption en-  
21  
22 ergy of  $-0.35$  eV. Experimental adsorption energies vary from  $-0.67$  eV to  
23  
24  $-0.41$  eV. These numbers are somewhat larger than our values. There could  
25  
26 be at least two explanations for that: (i) It is known that DFT is not capable  
27  
28 of describing the dispersion forces that might play a role in the interaction  
29  
30 between the water molecule and the surface. (ii) The experimental desorp-  
31  
32 tion temperatures and thus experimental adsorption energies correspond to  
33  
34 activation energies for desorption and not necessarily adsorption energies.  
35

36 It is common for these structures that the adsorption site is atop. There  
37  
38 is a small lateral displacement of the oxygen atom from the exact atop site  
39  
40 in the case of the symmetric and asymmetric adsorption geometry. That is  
41  
42 also ascertained on the Cu(100) and Cu(111) surfaces [19], [18]. We assumed  
43  
44 initially that water bounds to the surface through the oxygen atom which  
45  
46 was also confirmed in all of our calculations. The distance between oxygen  
47  
48 and the atop metal atom is  $2.2 \text{ \AA}$  for the symmetric geometry and  $2.1 \text{ \AA}$   
49  
50 for the asymmetric geometry. The most favorable adsorption geometries  
51  
52 are tilted with respect to the surface in agreement with experiments [8], [9]  
53  
54  
55  
56  
57  
58  
59  
60

1  
2  
3  
4 and [5] and almost all computational results. The tilting angle is  $71^\circ$  for  
5  
6 the symmetric adsorption geometry and  $80^\circ$  for the asymmetric adsorption  
7  
8 geometry. One of the OH-bonds is directed almost along the 'long' copper  
9  
10 row in the asymmetric geometry and there is no symmetry with respect to  
11  
12 the surface. The associated hydrogen atom directs to the surface. The other  
13  
14 bond directs away from the surface. In the symmetric adsorption geometry,  
15  
16 the water molecule and the surface possess one common symmetry plane and  
17  
18 both hydrogens point away from the surface. We found out that the most  
19  
20 favorable adsorption geometry is asymmetric with respect to the surface in  
21  
22 agreement with Mariani and Horn [10]. The calculated bond lengths  $0.976 -$   
23  
24  $0.981 \text{ \AA}$  and bond angle  $105.2 - 105.3^\circ$  of water on both adsorption geometries  
25  
26 are slightly increased compared to the calculated gas phase values of  $0.971 \text{ \AA}$   
27  
28 and  $104.6^\circ$ . Experimental values for the gas phase water are  $0.957 \text{ \AA}$  and  
29  
30  $104.5^\circ$ , respectively [36].

31  
32 For comparison, we also performed relaxations for the most favorable  
33  
34 upright adsorption geometry on the atop site. In this upright geometry, the  
35  
36 molecule is perpendicular with respect to the surface and all the atoms of the  
37  
38 molecule are right above the long copper row. The bond lengths  $0.973 \text{ \AA}$  are  
39  
40 slightly shorter than in the case of other adsorption geometries but there is a  
41  
42 significant increase in the bond angle which is  $108.5^\circ$ . The distance between  
43  
44 the surface and the oxygen atom is  $2.18 \text{ \AA}$ . The interaction between the  
45  
46 water molecule in the upright adsorption geometry and the surface is weaker  
47  
48 as the adsorption energy is only  $-0.27 \text{ eV}$ . All the structures are presented  
49  
50 in figure 2 and our best geometrical parameters for water on the Cu(110)  
51  
52 surface are presented in the Table 1. The asymmetric structure is similar  
53  
54  
55  
56  
57  
58  
59  
60

1  
2  
3  
4 to the one obtained earlier in a work where a DFT method with periodic  
5  
6 boundary conditions were also employed [21].  
7

8 The bonding of the water monomer to the metal surfaces is usually ex-  
9  
10 plained by the interaction between the dipole moment of the water molecule  
11  
12 and its induced dipole moment beneath the metal surface and the overlapping  
13  
14 of the d-orbitals of the metal surface and the lone pair orbitals of the water  
15  
16 molecule [1], [2]. The adsorption energy as small as  $-0.36$  eV in absolute  
17  
18 value indicates physisorption interaction. However, the tilted adsorption ge-  
19  
20 ometry points out to the formation of a chemical bound between the molecule  
21  
22 and the surface because upright geometry has been claimed to enhance the  
23  
24 dipole induced dipole interaction [18]. The  $1b_1$  and  $3a_1$  orbitals of the gas  
25  
26 phase water molecule are believed to be involved in bonding with the surface  
27  
28 whereas the  $2a_1$  and  $1b_2$  orbitals do not affect the bonding. The  $3a_1$  orbital is  
29  
30 in the symmetry plane of the molecule whereas the  $1b_1$  orbital is orthogonal  
31  
32 to the plane of the molecule. [2] Based on the symmetry arguments, inter-  
33  
34 action with the surface through the  $3a_1$  orbital is enhanced in the upright  
35  
36 adsorption geometry whereas the interaction through the  $1b_1$  orbital favors  
37  
38 the parallel geometry. Previous works on other copper planes [19], [18] give  
39  
40 similar results.

41 In order to analyze the interaction mechanism of the water molecule with  
42  
43 the copper surface, we computed the density of the states (DOS) for the  
44  
45 relaxed copper surface without the water molecule and for the symmetric  
46  
47 and asymmetric water-surface systems. For comparison, we also computed  
48  
49 the DOS for the most favorable upright adsorption geometry. To analyze  
50  
51 the observed changes in the DOS curves, we computed the local density of  
52  
53  
54  
55  
56  
57  
58  
59  
60

1  
2  
3  
4 the states (LDOS) of the adsorbed water molecule in symmetric, asymmetric  
5 and upright adsorption geometry and compared them with the density of the  
6 states of the gas phase molecule. We also computed the local densities of the  
7 states of the s, p and d orbitals of the copper atoms of the adsorption system  
8 and compared them with the corresponding LDOS of the bare metal slab.  
9  
10  
11  
12  
13  
14 [34]

15  
16 The DOS for the bare metal surface and the symmetric adsorption system  
17 are presented in figure 3. There are changes in regions around  $-22.5$  eV,  
18  $-10.3$  eV and  $-6.9$  eV due to adsorption as indicated with arrows. Analysis  
19 of the LDOS of the symmetric adsorption system revealed that the observed  
20 new peaks in figure 3 B correspond to the  $2a_1$ ,  $1b_2$  and  $3a_1$  orbitals of the  
21 water molecule. The peak that corresponds to the  $1b_1$  orbital of the gas  
22 phase water molecule was found to be hidden under the states of copper  
23 in the region around  $-5.1$  eV. The DOS and LDOS figures of asymmetric  
24 adsorption geometry are similar to the symmetric case expect the  $1b_2$  orbital  
25 where a small change is observed. Clear differences can be seen on the DOS  
26 and LDOS curves for upright adsorption geometry when compared with the  
27 other adsorption geometries.  
28  
29  
30  
31  
32  
33  
34  
35  
36  
37  
38  
39

40 To analyze the differences between the flat and upright adsorption ge-  
41 ometries we used the energy of the  $2a_1$  orbital as the zero-point energy of  
42 the systems because according to the literature the energetic position of the  
43  $2a_1$  orbital of the water molecule is not affected in the adsorption [1]. The  
44 LDOS for symmetric, asymmetric and upright adsorption geometry are pre-  
45 sented in figure 4. The vertical solid lines indicate approximate positions of  
46 the orbitals of gas phase water obtained in our calculations. In the upright  
47  
48  
49  
50  
51  
52  
53  
54  
55  
56  
57  
58  
59  
60

1  
2  
3  
4 geometry, the  $1b_1$  orbital is shifted 0.5 eV less and  $3a_1$  0.5 eV more from the  
5  
6 computed values for the gas phase water than the flat geometries. The de-  
7  
8 viation in the positions and the heights of the peaks indicates differences in  
9  
10 the bonding mechanism between flat and upright adsorption systems. For  
11  
12 comparison, we have experimental positions of experimental UPS spectra  
13  
14 peaks from references [10], [5] and [35]. They report the energetic positions  
15  
16 of the  $1b_2$ ,  $3a_1$  and  $1b_1$  orbitals only and because of that we chose to compare  
17  
18 the energetic differences of the experimental and computed peaks instead  
19  
20 of direct energies of the orbitals. Computed differences in the LDOS peaks  
21  
22 and the experimental ones are tabulated in the table 3 where fairly good  
23  
24 agreement of our calculated values with experimental values is seen.

25  
26 As seen from the figure 3a, the bare copper surface possesses no states  
27  
28 around the  $2a_1$  and  $1b_2$  states of water. Thus, these orbitals do not signifi-  
29  
30 cantly affect the bonding between the molecule and the metal surface. It is  
31  
32 common for all adsorption systems that the  $1b_2$  orbital remains practically  
33  
34 unchanged but the  $1b_1$  and  $3a_1$  orbitals are shifted to lower energies and  
35  
36 the LDOS peaks of the adsorption systems are usually smaller in energies  
37  
38 than the peaks of the gas phase water molecule. The LDOS of symmetric  
39  
40 and asymmetric adsorption geometries are almost identical and the energetic  
41  
42 position and the height of the  $1b_1$  orbital peak change most. The  $3a_1$  orbital  
43  
44 change most with the upright adsorption geometry. This indicates that the  
45  
46 flat adsorption geometry enhances interaction between the  $1b_1$  orbital and  
47  
48 the upright geometry enhances interaction with the  $3a_1$  orbital as expected  
49  
50 due to symmetry arguments. In addition, the analysis of the LDOS projected  
51  
52 on the s, p and d orbitals of copper of the bare surface and copper atoms of

1  
2  
3  
4 the adsorption systems revealed that the lone pair orbitals of water interact  
5  
6 with the d orbitals of the copper surface. Possible interaction with the p  
7  
8 orbitals of the copper surface was not observed.  
9

### 11 3.3 Vibrational analysis

12  
13  
14 For consistency, we wanted to use the same potential energy model for all  
15  
16 geometries. In order to minimize the number of data point computed for the  
17  
18 adsorbed geometries, where even single point energy calculations are time  
19  
20 consuming, we performed variational calculations for the gas phase water  
21  
22 with different potential energy functions and potential energy parameters  
23  
24 obtained with different number of data points. The convergence with respect  
25  
26 to different number of data points and terms in the potential energy functions  
27  
28 is shown in tabel 4.  
29

30 We assured that twelve data points in the vicinity of the minimum and  
31  
32 a simple potential energy function  $D_2y^2 + D_3y^3 + D_4y^4$  provides a sufficient  
33  
34 model. The results for the gas phase water are presented in the table 4.  
35  
36 We decided to use this computationally cheap treatment for the adsorption  
37  
38 geometries instead of more complicated models. The bond that directs to  
39  
40 the surface in the asymmetric adsorption geometry is an expectation. We  
41  
42 found out that there is an attractive interaction between the hydrogen atom  
43  
44 that directs to the metal surface. For that curve, we computed more data  
45  
46 points and also removed some data points where the H atom is too close to  
47  
48 the metal surface and fitted the points with a model with terms from  $y^2$  to  
49  
50  $y^{10}$ . The calculated wave numbers for the gas phase water are lower than  
51  
52 corresponding experimental values, as expected. See for example ref. [39].  
53  
54  
55

1  
2  
3  
4 The stretching potential energy curves of the isolated water molecule,  
5 symmetric, upright and asymmetric adsorption geometry are presented in  
6 figure 5. The stretching curves for the bonds in the symmetric and upright  
7 adsorption geometry and the bond of the asymmetric adsorption geometry  
8 that points away from the surface are identical. A significant lowering of  
9 the dissociation energy occurs with the bond of the asymmetric geometry  
10 that is directed to the metal surface. The bond is a bit longer than the  
11 others and there is an attractive interaction with the copper surface. All the  
12 adsorption geometries possess lower dissociation energies than the gas phase  
13 molecule. The parameters for the potential energy surfaces are in table 5 and  
14 the calculated vibrational wave numbers in table 6 where the experimental  
15 wave numbers for the gas phase water are also given.  
16  
17  
18  
19  
20  
21  
22  
23  
24  
25  
26

27  
28 The wave numbers of the stretching modes of the adsorption geometries  
29 are lower than the corresponding gas phase values. The wave numbers of the  
30 stretching modes of the upright geometry are closer to the gas phase values  
31 than the corresponding wave numbers of the flat geometries due to a weaker  
32 interaction with the metal surface. Otherwise, the spectral positions are sim-  
33 ilar to the symmetric adsorption case. The different interaction mechanism  
34 of the symmetric and upright geometry does not seem to have significant  
35 influence on the spectral positions as the largest differences are between the  
36 wave numbers of the symmetric and asymmetric structure where the inter-  
37 action mechanisms are similar. This could have been expected beforehand  
38 because the stretching motion of the water molecule changes mainly the po-  
39 sitions of the hydrogen atoms and has little effect on the lone pair orbitals.  
40 The experimental OH- stretching region of the spectra of the adsorbed water  
41  
42  
43  
44  
45  
46  
47  
48  
49  
50  
51  
52  
53  
54  
55  
56  
57  
58  
59  
60

1  
2  
3  
4 molecule is broad with a full width at half maximum of  $400 - 450 \text{ cm}^{-1}$  even  
5  
6 at low temperatures. It can be resolved into three components at  $3180 \text{ cm}^{-1}$ ,  
7  
8  $3375 \text{ cm}^{-1}$  and  $3600 \text{ cm}^{-1}$ . They have been explained by three kinds of OH-  
9  
10 bonds: bonded to the surface, hydrogen bonded and free bonds, respectively  
11  
12 [8]. All our computed values for the stretching fundamentals are in the middle  
13  
14 of the experimental stretching region bands particularly when the expected  
15  
16 deviation of  $100 \text{ cm}^{-1}$  is taken into account. The surface selection rule [38]  
17  
18 implies that only modes with an oscillating dipole perpendicular to the metal  
19  
20 surface are infra red (IR) active. The detailed analysis of the intensities of  
21  
22 the different transitions would require computing the dipole moment surface  
23  
24 of the system, which, in this case, is not a well-defined problem due to the  
25  
26 periodic boundary conditions employed to a metallic system. We decided to  
27  
28 estimate the intensities of the reported transitions by using the dipole mo-  
29  
30 ment transitions vectors for the gas phase water [37] and projecting them on  
31  
32 the axis perpendicular to the surface. It was found out that the asymmetric  
33  
34 modes of the symmetric and upright geometries are IR inactive, all the sym-  
35  
36 metric modes and the mode (100) of the asymmetric structure possess similar  
37  
38 intensities and the (010) mode of the asymmetric structure is more intensive  
39  
40 than the others (see table 6 for labeling the states). Symmetric vibrations of  
41  
42 the symmetric and upright geometry correspond to the 'free OH-bond case'  
43  
44 reported in experimental works. The interpretation of the vibrations of the  
45  
46 asymmetric structure is not evident. The eigenfunctions of the vibrational  
47  
48 states showed that the bond directed away from the surface is responsible for  
49  
50 the vibration with wave number  $3560 \text{ cm}^{-1}$  and the wave number  $3347 \text{ cm}^{-1}$   
51  
52 corresponds to the bond directed to the surface. The peak at  $3180 \text{ cm}^{-1}$   
53  
54  
55  
56  
57  
58  
59  
60

1  
2  
3  
4 seen in the spectra has previously been assigned to the OH-bond directed  
5 to surface. According to our calculations, bonding to the surface decreases  
6 the wave number of the stretch but the decrease is not that large. Actually,  
7 our computed value is closer to the peak around  $3375\text{ cm}^{-1}$  that according  
8 to Lackey corresponds to hydrogen-bonded OH-bonds [8].  
9

10  
11  
12  
13  
14 The bending mode for adsorbed water has been observed around  $1600\text{ cm}^{-1}$   
15 [8], which is the same value as for the gas phase water molecule. Our com-  
16 puted values are lower than the computed gas phase values by more than  
17  $30\text{ cm}^{-1}$ . Hydrogen bonding is possibly seen in the experimental results be-  
18 cause according to Thiel [1] the interaction with the surface decreases the  
19 wave numbers for bending but the hydrogen bonding increases it. Clustering  
20 of the water molecule is assumed to occur on the Cu(110) surface even if the  
21 coverage is small [8]. Bending wave number decrease in adsorption has also  
22 been reported by Ribarsky [22], although his harmonic normal mode analysis  
23 was based on a five-atomic cluster model.  
24  
25  
26  
27  
28  
29  
30  
31  
32  
33  
34  
35

## 36 4 Conclusions

37  
38  
39 We have studied adsorption of water on the Cu(110) surface using the den-  
40 sity functional theory with the slab model. We have found out that water  
41 bounds to the atop site with a weak chemisorption bond between the lone  
42 pair orbitals of the oxygen atom and the d orbitals of the metal atoms. The  
43 most favorable adsorption site is atop and the adsorption geometry is tilted  
44 and asymmetric with respect to the surface in agreement with experimental  
45 results and previous similar computational works. The calculated orbital en-  
46 ergies for the tilted geometries are similar to the experimental ones, which  
47  
48  
49  
50  
51  
52  
53  
54  
55

1  
2  
3  
4 also confirms that the adsorption geometry of water is tilted. Adsorption  
5  
6 energies are around  $-0.36$  eV. Experimental adsorption energies vary from  
7  
8  $-0.67$  to  $-0.41$  eV depending on the interpretation of the desorption tem-  
9  
10 peratures.

11  
12 We have computed vibrational transitions using a model where the Hamil-  
13  
14 tonian for the vibrational motion have been constructed and its eigenvalues  
15  
16 have been computed variationally. The work is based on the adiabatic ap-  
17  
18 proximation where there is no coupling of the internal vibrational modes of  
19  
20 the molecule with the frustrated translations and rotations or to the phonon  
21  
22 modes of the surface. Without the adiabatic assumption the computed posi-  
23  
24 tions of the spectral peaks for the adsorbed geometries would have splittings  
25  
26 which in addition to clustering are seen as broadening in the experimental  
27  
28 spectra. In principle, it is possible to compare the wave numbers computed in  
29  
30 different adsorption geometries with the experimental spectra and to make  
31  
32 conclusions about the possible adsorption geometry of the molecule. This  
33  
34 is potentially important when the interpretation of the experimental results  
35  
36 is difficult due to broad spectra caused by many simultaneous adsorption  
37  
38 geometries or clustering.

39  
40 Our computed density-functional wave numbers have deviations from the  
41  
42 experimental wave numbers more than  $100\text{ cm}^{-1}$  for the stretches and  $50\text{ cm}^{-1}$   
43  
44 for the bending mode. Luckily, the differences between adsorbed geometries  
45  
46 and gas phase structures are produced better. The wave numbers of the  
47  
48 adsorbed water molecule are lower than the gas phase values which indicates  
49  
50 softening of the bonds. It may explain why water is assumed to dissociate  
51  
52 on the surface and why it is more reactive when the molecule adsorbs. For  
53  
54  
55

1  
2  
3  
4 example, lowering of the dissociation energy is easily seen from the stretching  
5  
6 potential energy curves. The interaction mechanism does not have large  
7  
8 effect on the vibrational wave numbers. However, when the interaction is  
9  
10 the weakest, the wave numbers are closer to experimental values. The bond  
11  
12 directed to the metal surface produces lower stretching fundamental wave  
13  
14 number than the others which support the experimental assumption that  
15  
16 the lowest peak of the stretching region is associated with the bonds directed  
17  
18 to the surface.  
19

## 20 21 22 **Acknowledgments** 23

24  
25 We would like to thank CSC Scientific Computing Ltd for providing computer  
26  
27 time and Magnus Ehrnrooth Foundation for financing the project. Labora-  
28  
29 tory of Physical Chemistry has been a part of The Center of Excellence in  
30  
31 Computational Molecular Science funded by the Academy of Finland and  
32  
33 University of Helsinki during part of the work.  
34  
35  
36  
37  
38  
39  
40  
41  
42  
43  
44  
45  
46  
47  
48  
49  
50  
51  
52  
53  
54  
55  
56  
57  
58  
59  
60

## References

- [1] P. A. Thiel, T. E. Madey. *Surf. Sci. Rep.*, **7**, 211 (1987).
- [2] M. Henderson. *Surf. Sci. Rep.*, **46**, 1 (2002).
- [3] K. Morgenstern, K. Rieder. *J. Chem. Phys.*, **116**, 13 5746 (2002)
- [4] R. Smith, D. Killelea, D. DelSesto, A. Utz. *Science*, **304**, 5673 992 (2004).
- [5] A. Spitzer, H. Lüth. *Surf. Sci.*, **120**, 376 (1988).
- [6] M. Polak. *Surf. Sci.*, **321**, 249 (1994).
- [7] G. Mariani, K. Horn. *Surf. Sci.*, **126**, 279 (1983), Bange, K., R. Döhl, D.E. Grider, J.K. Sass. *Vacuum*, **33**, 10 757 (1983), K. Bange, D. E. Grider, T. E. Madey, J. K. Sass. *Surf. Sci.*, **136**, 38 (1984) and A. Spitzer, H. Lüth. *Surf. Sci.*, **120**, 376 (1988).
- [8] D. Lackey, J. Schott, B. Straehler, J. Sass. *J. Chem. Phys.*, **91**, 2 1365 (1989)
- [9] S. Andersson, C. Nyberg, C. Tengstål. *Chem. Phys. Lett.*, **104**, 4 305 (1984)
- [10] G. Mariani, K. Horn. *Surf. Sci.*, **126**, 279 (1983).
- [11] D. Lackey, J. Schott, B. Straehler, J. Sass. *J. Chem. Phys.*, **91**, 2 1365 (1989), K. Andersson, A. Gomez, C. Glover, D. Nordlund, H. Öström, T. Schiros, O. Takahashi, H. Ogasawara, L. G. M. Pettersson, A. Nilsson. *Surf. Sci. Lett.*, **585**, L183 (2005). Bange, K., R. Döhl, D.E. Grider, J.K. Sass. *Vacuum* **33**, 10 757 (1983), K. Bange, D. E. Grider, T. E. Madey,

- 1  
2  
3  
4 J. K. Sass. *Surf. Sci.*, **136**, 38 (1984), *Electrochim. Acta*, **36**, 11/12 1883  
5  
6 (1991).  
7  
8  
9 [12] J. Sass, D. Lackey, J. Schott. *Electrochim. Acta*, **36**, 11/12 1883 (1991).  
10  
11 [13] A. Carley, P. Davies, M. Roberts, K. Thomas. *Surf. Sci. Lett.*, **238**,  
12 L467 (1990).  
13  
14  
15 [14] T. Sueyoshi, T. Sasaki, Y. Iwasawa. *J. Phys. Chem. B*, **101**, 4648 (1997)  
16  
17  
18 [15] H. Ruuska, T. Pakkanen, R. Rowley. *J. Chem Phys. B*, **108**, 13 2614  
19 (2004).  
20  
21  
22 [16] A. Ignaczak, J. A. N. F. Gomes. *J. Electroan. Chem.*, **420**, 209 (1997).  
23  
24  
25 [17] G. C. Wang, L. Jiang, X. Y. Pang, Z. S. Cai, Y. M. Pan, X. Z. Zhao, Y.  
26 Morikawa, J. Nakamura. *Surf. Sci.*, **543**, 118 (2003).  
27  
28  
29 [18] A. Michaelides, V. A. Ranea, P. L. de Andres, D. A. King. *Phys. Rev.*  
30 *Lett.*, **90**, 21 216102 (2003).  
31  
32  
33 [19] S. Wang, Y. Cao, P. A. Rikvold. *Phys. Rev. B*, **70**, 205410 (2004).  
34  
35  
36 [20] S. Izvekov, A. Mazzolo, K. VanOpdorp, G. A. Voth. *J. Chem. Phys.*,  
37 **114**, 7 3248 (2001).  
38  
39  
40 [21] Q.-L. Tang, Z.-X. Chen, *Surf. Sci.* doi: 10.1016/j.susc.2006.11.036  
41 (2006).  
42  
43  
44 [22] M. Ribarsky, W. Luedtke, U. Landman. *Phys. Rev. B*, **32**, 2 1430 (1985).  
45  
46  
47 [23] J. Pesonen, L. Halonen. *Adv. Chem. Phys.*, **125**, 269 (2003).  
48  
49  
50  
51  
52  
53  
54  
55  
56  
57  
58  
59  
60

- 1  
2  
3  
4 [24] H. Wei, T. Carrington. *J. Chem. Phys.*, **97** 5, 3029 (1992).  
5  
6  
7 [25] M. Born, K. Huang. *Dynamical theory of Crystal lattices*. Oxford at the  
8 Clarendon press (1956).  
9  
10  
11 [26] T. Kurten, M. Biczysko, T. Rajamäki, K. Laasonen, L. Halonen. *J.*  
12 *Phys. Chem. B*, **109** (18), 8954-8960 (2005).  
13  
14  
15 [27] G. Kresse, J. Hafner. *Phys. Rev. B*, RC558 (1993) and G. Kresse, J.  
16 Furthmüller. *Comput. Mat. Sci.*, **6**, 15 (1996); *Phys. Rev. B*, **54**, 11169  
17 (1996).  
18  
19  
20  
21  
22 [28] G. Kresse, D. Joubert. *Phys. Rev. B*, **59**, 3 1758 (1999).  
23  
24  
25 [29] N. Ashcroft, N. Mermin. *Solid State Physics*, (Saunders College,  
26 Philadelphia (1981).  
27  
28  
29  
30 [30] A. R. Hoy, I. M. Mills, G. Strey. *Mol. Phys.*, **24**, 1265 (1972).  
31  
32  
33 [31] E. Kauppi, L. Halonen. *J. Phys. Chem.*, **94**, 5779 (1990).  
34  
35  
36 [32] A. H. Stroud. *Gaussian Quadrature Formulas*, Prentice-Hall, Inc, En-  
37 glewood Cliffs, N.J. (1966).  
38  
39  
40 [33] G. Mariani, K. Horn. *Surf. Sci.*, **126**, 279 (1983), D. Lackey, J. Schott,  
41 B. Straehler, J. Sass. *J. Chem. Phys.*, **91**, 2 1365 (1989), Bange, K., R.  
42 Döhl, D.E. Grider, J.K. Sass. *Vacuum*, **33**, 10 757 (1983), K. Bange, D. E.  
43 Grider, T. E. Madey, J. K. Sass. *Surf. Sci.*, **136**, 38 (1984), A. Spitzer, H.  
44 Lüth. *Surf. Sci.*, **120**, 376 (1988), M. Polak. *Surf. Sci.*, **321**, 249 (1994).  
45  
46  
47  
48  
49  
50  
51 [34] We have used the programs p4V and LEV00 as tools to  
52 analyze the charge density and density of the states of the  
53  
54  
55  
56  
57  
58  
59  
60

1  
2  
3  
4 molecule. See <http://cms.mpi.univie.ac.at/odubay/p4vasp/> and  
5  
6 <http://www.cmmp.ucl.ac.uk/lev/codes/lev00/> for details.  
7

8  
9 [35] Bange, K., R. Döhl, D.E. Grider, J.K. Sass. *Vacuum*, **33**, 10 757 (1983).

10  
11 [36] J. Tennyson, N. F. Zobov, R. Williamson, O. L. Polyansky. *J. Phys.*  
12 *Chem., Ref. Data.* **30**, 3 735 (2001).  
13

14  
15 [37] U. Jørgensen, P. Jensen. *J. Mol. Spect.*, **161**, 219 (1993).  
16

17  
18 [38] N. Sheppard, J. Erkelens. *Appl. Spect.*, **38** 4, 471 (1984).  
19

20  
21 [39] J. Sauer, P. Ugliengo, E. Garrone, R. Saunders. *Chem. Rev.* **94**, 2095  
22  
23 (1994)  
24  
25  
26  
27  
28  
29  
30  
31  
32  
33  
34  
35  
36  
37  
38  
39  
40  
41  
42  
43  
44  
45  
46  
47  
48  
49  
50  
51  
52  
53  
54  
55  
56  
57  
58  
59  
60

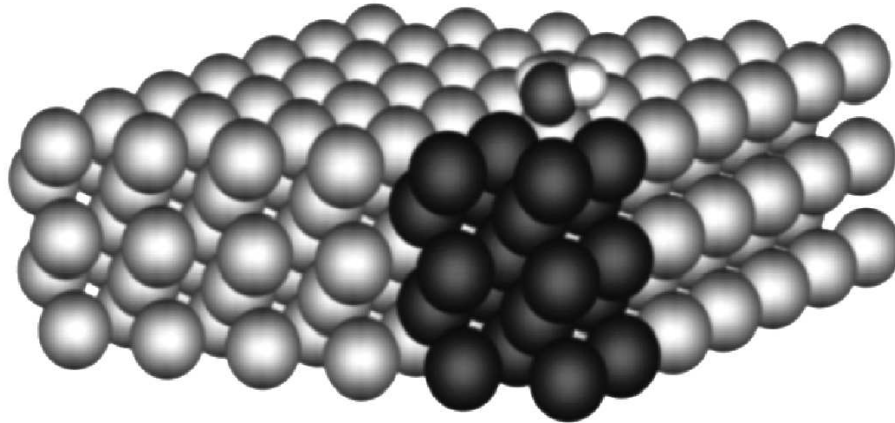


Figure 1: The slab model. Dark atoms represent atoms in one super cell.

Peer Review Only

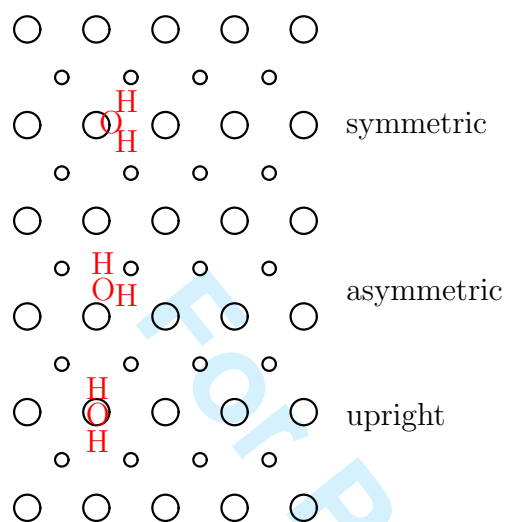


Figure 2: Symmetric, asymmetric and upright adsorption geometry

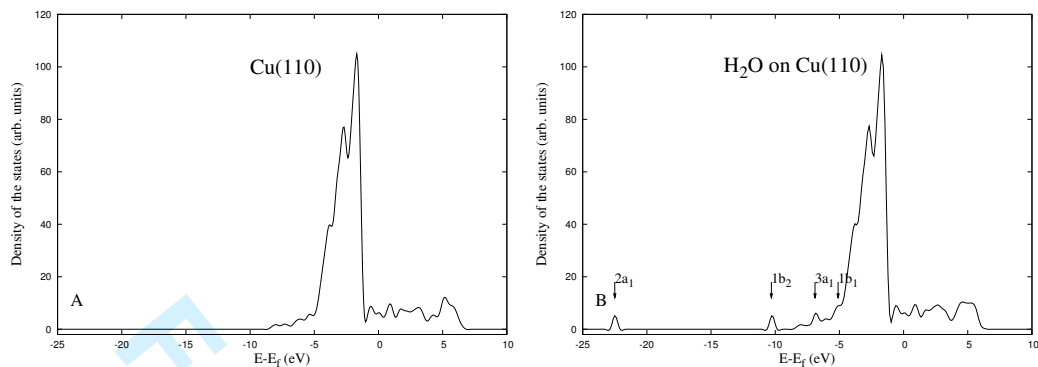


Figure 3: (A) Density of the states (DOS) of the Cu(110) surface. (B) Density of the states in the symmetric adsorption system of water and the Cu(110) surface. The arrows point DOS-peaks that are due to adsorption.

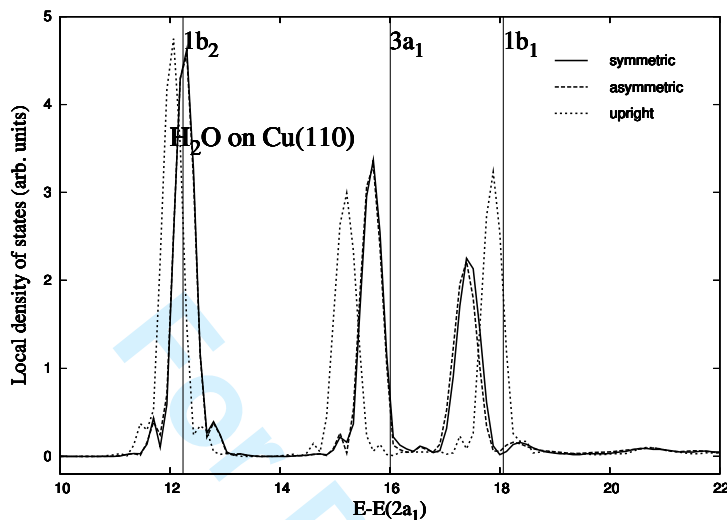


Figure 4: Local density of the states (LDOS) of the symmetric, asymmetric and upright adsorption systems and density of the states of the water molecule. The DOS curves for the symmetric and asymmetric adsorption geometries are almost identical except for the lowest molecular orbital around  $-5$  eV where a small difference can be seen. The arrows represent the approximate positions of the molecular orbitals of the gas phase water molecule. Energies are given in eV. The energy axes in this figure is chosen such that the energetic position of the  $2a_1$  orbital is set to zero.

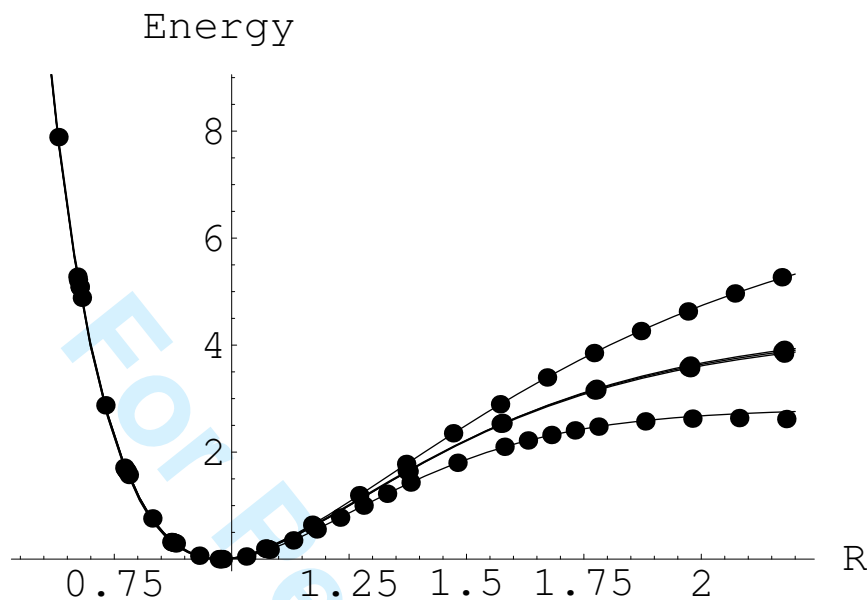


Figure 5: Potential energy curves for stretching. The topmost curve corresponds to the gas phase water. The curves for the symmetric and upright adsorption geometry are one on the other with the the bond of the asymmetric structure that directs away from the surface. The lowest curve corresponds to the bond of the asymmetric structure that is directed to the surface. Energy is given in eV and the bond length  $R$  in Å.

size of the super cell	$E_{\text{ads}}$ (eV)	$r_{\text{OH}}$ (Å)	$\theta$ (deg)	$r_{\text{CuO}}$ (Å)	$\phi$ (deg)
2 × 2 slab, 5 layers 10 Å vacuum	-0.35	0.976	105.3	2.23	71.3
3 × 3 slab, 5 layers 10 Å vacuum	-0.35	0.976	105.7	2.20	65.8
2 × 2 slab, 7 layers 10 Å vacuum	-0.35	0.976	105.3	2.23	72.3
2 × 2 slab, 9 layers 10 Å vacuum	-0.36	0.976	105.4	2.22	71.4
2 × 2 slab, 5 layers 15 Å vacuum	-0.34	0.977	105.2	2.24	74.8

Table 1: The result of the convergence test with respect to the size of the super cell

	gas phase	symmetric	asymmetric	upright
$r_A(\text{\AA})$	0.971	0.976	0.976	0.973
$r_B(\text{\AA})$	0.971	0.976	0.981	0.973
$\theta_e(\text{deg})$	104.6	105.3	105.2	108.5
$r_{\text{CuO}}(\text{\AA})$	-	2.23	2.14	2.18
$\phi(\text{deg})$	-	71.3	79.7	90
$E_a$ (eV)	-	-0.35	-0.36	-0.27

Table 2: The quantities  $r_A$  and  $r_B$  are the bond lengths and  $\theta_e$  is the bond angle of the water molecule,  $r_{\text{CuO}}$  is the distance between the oxygen atom and the copper atom below it,  $\phi$  is the angle between the surface normal and the water plane and  $E_a$  is the adsorption energy as defined in the text.

	gas phase (exp)	symmetric	asymmetric	upright	exp
$E(1b_1) - E(3a_1)$ (eV)	2.1 (2.1)	1.7	1.8	2.7	1.6–2.0
$E(3a_1) - E(1b_2)$ (eV)	3.8 (3.9)	3.4	3.3	3.1	3.8–4.2

Table 3: The separation of the  $1b_1$  and  $3a_1$  and  $3a_1$  and  $1b_2$  peaks in computed LDOS curves and corresponding values from references [10], [35] and [5]. Experimental values in the parenthesis have been taken from the reference [35]

number of the data points	12	28	28
model	$D_2y^2 + D_3y^3 + D_4y^4$	$D_2y^2 + D_3y^3 + D_4y^4$	from $y^2$ to $y^{10}$
$(00)_{+1}$	1545	1545	1545
$(10)_{+0}$	3555	3552	3550
$(10)_{-0}$	3649	3647	3642

Table 4: The convergence with respect to the potential energy surface model and the choice of the parameters. Wave numbers are given in  $\text{cm}^{-1}$ .

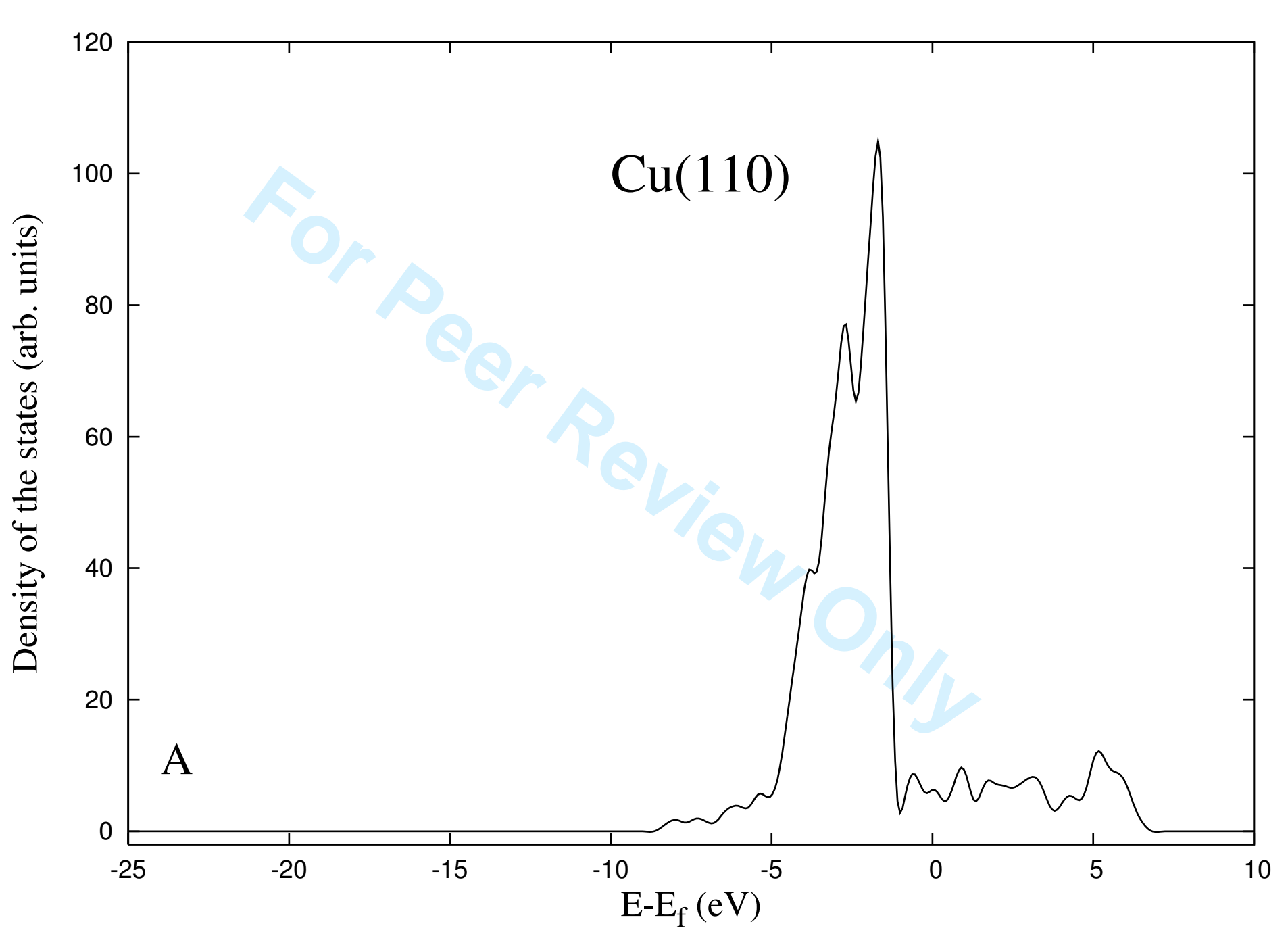
See table 6 for the labeling the states. In the model on the right hand side, the Morse parameter  $a$  has been constrained to the value obtained from the model  $D_2y^2 + D_4y^4$  and the data points have then fitted into a model that contains all potential energy terms from  $y^2$  to  $y^{10}$ .

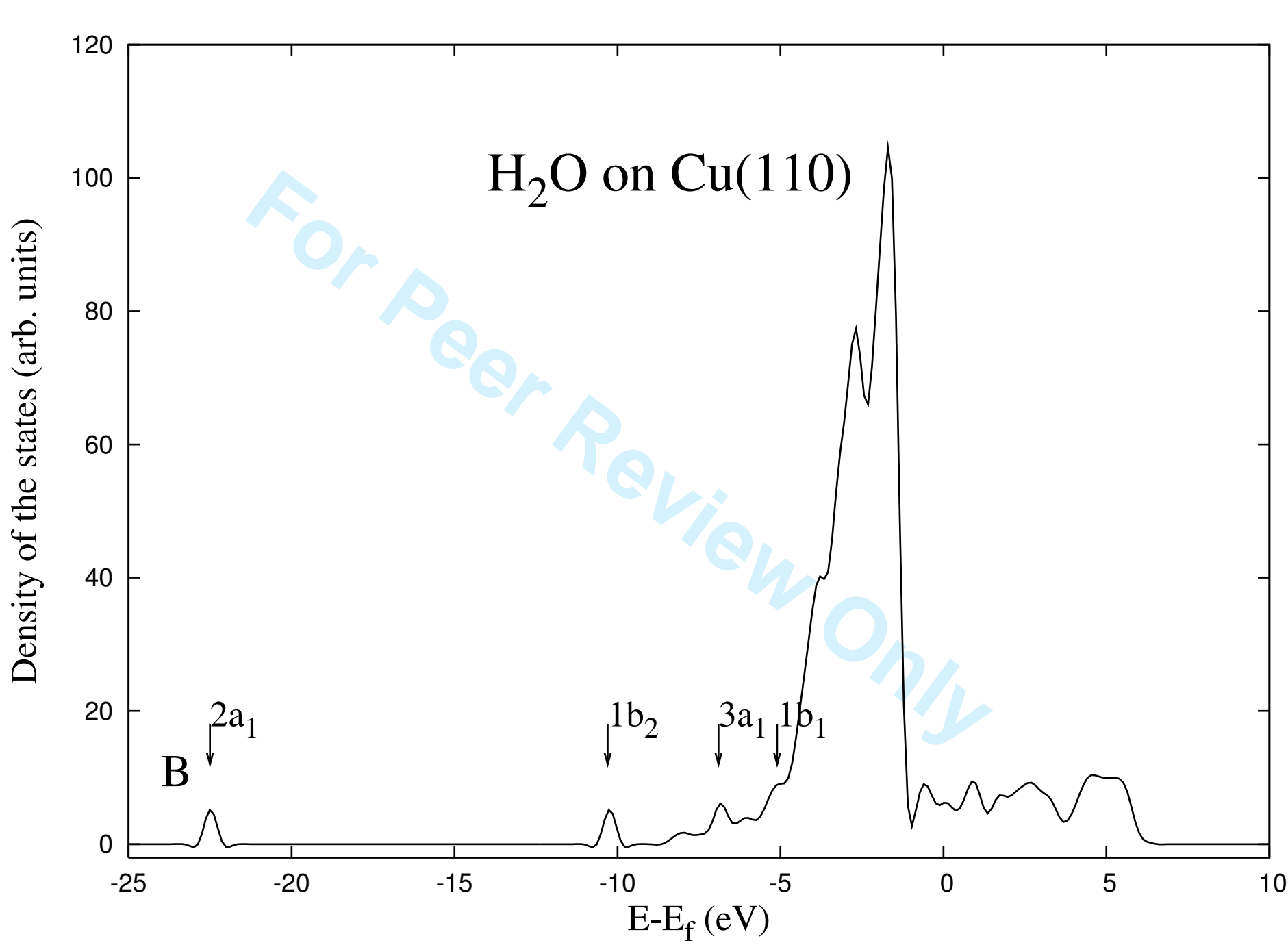
parameter	gas phase	symmetric	upright	asymmetric
$a$ ( $\text{\AA}^{-1}$ )	1.4501	2.49258	2.42155	2.42642
$D_2$ (aJ)	1.4501	0.637031	0.681347	0.671124
$D_3$ (aJ)	-0.670345	-0.0177527	-0.0146682	–
$D_4$ (aJ)	0.344533	0.032307	0.0305745	0.0329666
$a'$ ( $\text{\AA}^{-1}$ )				2.64959147
$D'_2$ (aJ)				0.513237
$D'_3$ (aJ)				0.013466
$D'_4$ (aJ)				0.0282639
$f_{rr'}$ ( $\text{aJ}\text{\AA}^{-2}$ )	-0.0948686	-0.0725689	-0.105353	-0.0668896
$f_{\theta\theta}$ ( $\text{aJ rad}^{-2}$ )	0.678738	0.656309	0.612189	0.64792
$f_{\theta\theta\theta}$ ( $\text{aJ rad}^{-3}$ )	-0.846216	-0.817509	0.784897	-0.8086
$f_{\theta\theta\theta\theta}$ ( $\text{aJ rad}^{-4}$ )	-0.426945	-0.39709	-0.272521	-0.351787
$f_{r\theta}$ ( $\text{aJ}\text{\AA}^{-1}\text{ rad}^{-1}$ )	0.27246	-0.241484	0.233361	0.251393
$f_{r\theta\theta}$ ( $\text{aJ}\text{\AA}^{-1}\text{ rad}^{-2}$ )	-0.24166	-0.294004	-0.293499	-0.267818
$f_{rr\theta}$ ( $\text{aJ}\text{\AA}^{-2}\text{ rad}^{-1}$ )	-0.234299	-0.26423	-0.12719	-0.235541
$f_{r'\theta}$ ( $\text{aJ rad}^{-1}$ )				0.192319
$f_{r'\theta\theta}$ ( $\text{aJ}\text{\AA}^{-1}\text{ rad}^{-2}$ )				-0.393742
$f_{r'r'\theta}$ ( $\text{aJ}\text{\AA}^{-2}\text{ rad}^{-1}$ )				-0.399861

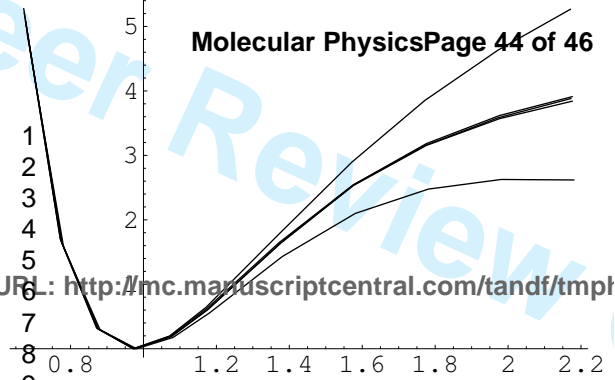
Table 5: The numerical values of the parameters from the fit of the calculated potential energy points on the potential energy function. The coefficients of terms from  $y^5$  to  $y^{10}$  that were used for the bond directed to the surface in the asymmetric structure are not shown.

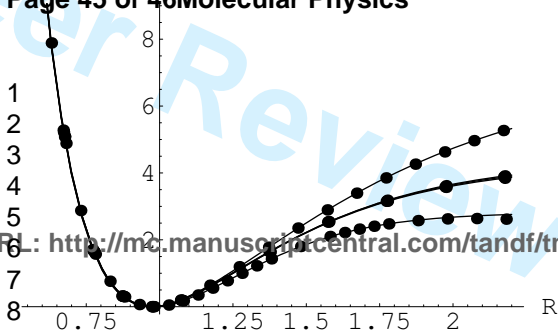
local	gas phase	gas phase exp	symmetric	upright	local	asymmetric
(00) <sub>+1</sub>	1545	1595	1514	1469	001	1499
(00) <sub>+2</sub>	3051	3152	2990	2899	002	2958
(10) <sub>+0</sub>	3555	3657	3491	3507	100	3347
(10) <sub>-0</sub>	3649	3756	3578	3618	010	3560
(10) <sub>+1</sub>	5089	5235	4991	4961	101	4823
(10) <sub>+1</sub>	5185	5331	5080	5075	011	5046
(20) <sub>+0</sub>	7005	7202	6822	6872	200	6480
(20) <sub>-0</sub>	7049	7250	6822	6922	110	6851
(11) <sub>+0</sub>	7236	7445	7090	7161	020	6959

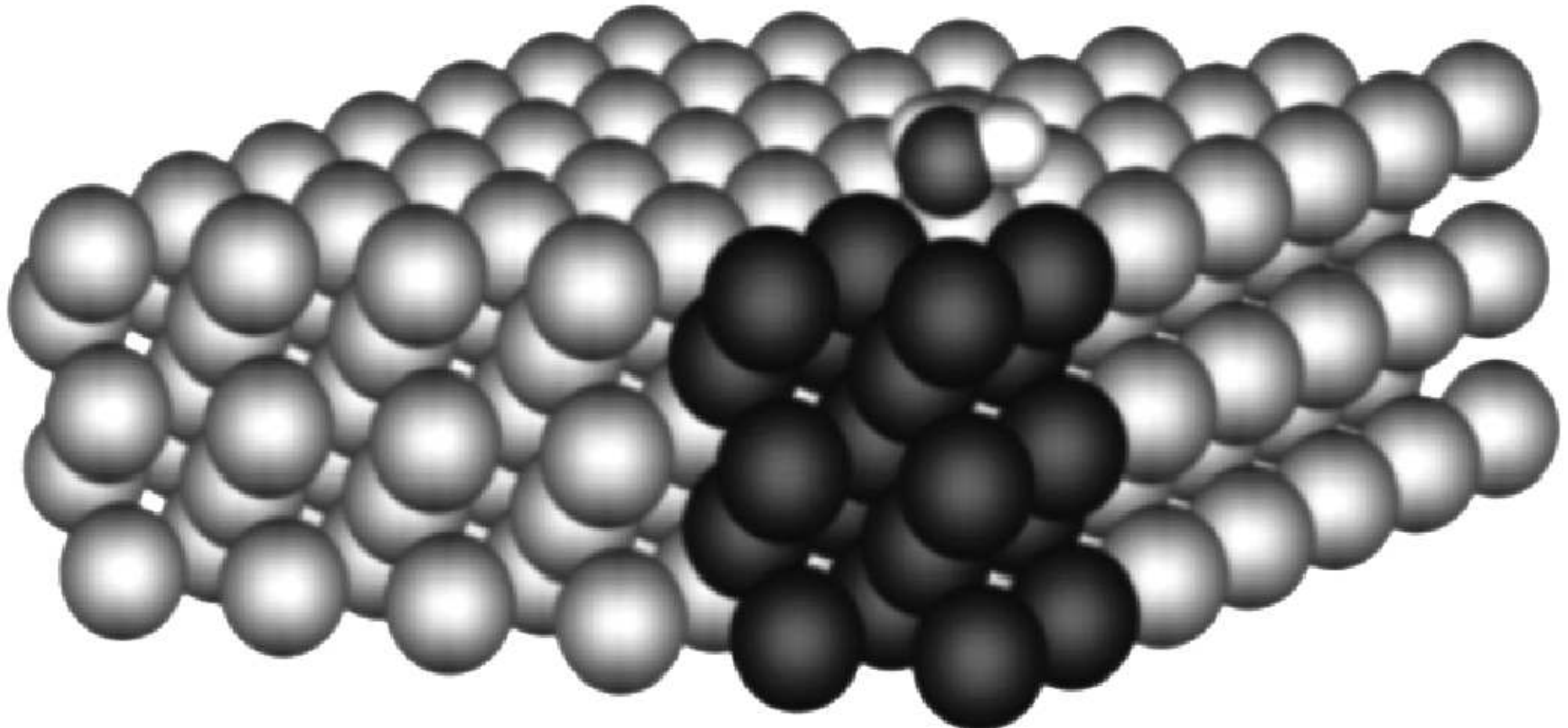
Table 6: The vibrational transitions of the isolated water monomer and the water monomer adsorbed on the Cu(110) surface. Experimental values are from reference [36]. All values are given in  $\text{cm}^{-1}$ . Local mode assignments of the transitions have been used for all the structures. Two numbers in the quantum labels express two OH bonds and the third number indicates the number of bending quanta. For symmetric structures, we denote symmetric vibration by + and asymmetric vibration by -.











URL: <http://mc.manuscriptcentral.com/tandf/tmph>

1  
2  
3  
4  
5  
6  
7  
8  
9  
10  
11  
12  
13  
14  
15  
16  
17  
18  
19  
20  
21  
22  
23  
24  
25  
26  
27  
28  
29  
30  
31  
32  
33